Signal processing techniques for nonlinear structural dynamical systems

C Pezeshki and W H Miles

Department of Mechanical and Materials Engineering,

and S Elgar

Department of Electrical and Computer Engineering,
Washington State University, Pullman WA 99164-2920

Various signal processing techniques are introduced into the structural dynamics literature, notably higher-order spectra for steady-state response and wavelet transforms for transient response of systems. The structural behavior of the buckled beam, modeled by the one-mode Galerkin approximation is examined to demonstrate the utility of the techniques. Higher-order spectra illuminate nonlinear energy coupling mechanisms in the frequency domain for the steady state response. Wavelet transforms show the development of the frequency spectrum in the transient portion of the response.

INTRODUCTION

The magnetically buckled beam has been studied by a variety of authors [Moon and Holmes, 1979], [Dowell and Pezeshki, 1986] and behavior for the one spatial mode Galerkin reduction of the beam, otherwise known as Duffing's equation with a negative linear stiffness, is well documented. When excited by a sinusoidal force, the beam's motion is described by

$$\ddot{A} + \gamma\dot{A} - \tfrac{1}{2}(A - A^3) = F_o \sin\Omega t \qquad (1)$$

where A is the displacement at the tip of the beam, γ is the damping coefficient, the excitation force has amplitude F_o and frequency Ω, and the overdot represents differentiation with respect to time. Duffing's equation and the buckled beam exhibit phenomena such as period doubling and chaotic oscillations.

The magnetically buckled beam is often referred to as a two- well potential problem. At rest, the physical system has two stable equilibria, one buckled about the left magnet, the other about the right magnet. The beam also has one unstable equilibrium, located about the center of the two magnets. If excited with a small sinusoidal force, the beam will oscillate about one of the two stable equilibria in a roughly sinusoidal fashion. However, when the force amplitude is raised to a sufficient level, the beam will jump back and forth between the two static equilibria, in effect "snapping through" the centerline of the system.

To demonstrate the use of cross-bispectral analysis, the Duffing equation excited by a multifrequency excitation is examined, represented by the following equation,

$$\ddot{A} + \gamma\dot{A} - \tfrac{1}{2}(A - A^3) = F_o \sin\Omega t + F_o \sin(2\Omega t + \phi) \qquad (2)$$

Systems with cubic nonlinearities, including some with two- frequency excitation, have been investigated previously [Plaut et al, 1986], [Zavodney et al, 1989]. The present study investigates methods of quenching chaotic motion by varying the phase angle ϕ of the forcing term in Eq (2), and using cross-bispectral analysis for insight into the rationale for system behavior. For demonstration of the use of the wavelet transform, Eq (1) is considered. The system with small damping is discussed, a sample trajectory is calculated, and the transform is applied.

BISPECTRAL ANALYSIS AND NUMERICAL DETAILS

Details and applications of bispectral analysis can be found in references [Hassleman et al, 1963], [Kim and Powers, 1979], [Nikias and Raghuveer, 1987], [Haubrich, 1965]. A brief description is presented here for completeness .

For a discretely sampled time series $\eta(t)$ with the Fourier representation

$$\eta(t) = \sum_n C(\omega_n) \exp(i\omega_n t) + C^*(\omega_n) \exp(-i\omega_n t), \qquad (3)$$

the power, auto- and cross-bicoherence spectra (normalized bispectra) are defined as

$$P(\omega_n) = E[C(\omega_n)C^*(\omega_n)] \qquad (4)$$

$$B(\omega_1,\omega_2) = \frac{E[C(\omega_1)C(\omega_2)C^*(\omega_1+\omega_2)]}{P(\omega_1)P(\omega_2)P(\omega_1+\omega_2)} \qquad (5)$$

$$XB_{jk}(\omega_1,\omega_2) = \frac{E[C_i(\omega_1)C_j(\omega_2)C_k^*(\omega_1+\omega_2)]}{P_j(\omega_1)P_j(\omega_2)P_k(\omega_1+\omega_2)} \qquad (6)$$

respectively, where ω_n is the radian frequency, the subscript n is a frequency index, the C's are the complex Fourier coefficients of the time series, an asterisk indicates complex conjugate, and $E[\ ]$ is the expected-value, or average, operator. The subscripts j,k in (6) indicate separate time series; in the cases considered here, input and output, respectively. Rewriting the complex Fourier coefficients as $C(\omega_n) = c_n\exp(i\Phi_n)$, the bispectrum becomes

$$B(\omega_1,\omega_2) = E[c_1c_2c_{1+2}\exp\{i(\Phi_1+\Phi_2-\Phi_{1+2})\}]. \quad (7)$$

If the three modes of the triad are independent of each other (ie, Φ_1,Φ_2,Φ_{1+2} are random phases), then, when averaged over many realizations, the triple products in (5-7) will be zero. On the other hand, if the modes at frequencies ω_1, ω_2, and $\omega_1+\omega_2$ are quadratically coupled, the biphase $\Phi_1+\Phi_2-\Phi_{1+2}$ will be nonrandom even if Φ_1 and Φ_2 are randomly varying. Thus, the bispectrum will be nonzero. Consequently, the bicoherence indicates the relative amount of quadratic phase coupling between the three modes in a triad.

WAVELET TRANSFORMS

Recently, much attention has been directed in the electrical engineering and applied mathematics communities towards the use of wavelet transforms [Grossman et al, 1989], [Meyer, 1989], [Daubechies, 1989], [Flandrin and Rioul, 1990], [Arneodo and Grasseau, 1988], [David and Chapron, 1990]. Wavelet transforms can be defined as a new type of formalism of signal energy representation depending on time and scale [Flandrin and Rioul, 1990]. Because of their unique properties involving their scalability, they can be used very successfully to study fractal signals, nonstationary phenomena, and other signals not tractable to ordinary Fourier analysis [Arneodo and Grasseau, 1988]. The definition of the wavelet transform, as given by Grossman[1989], is

$$S(b,a) = a^{-1/2}\int g^*[(t-b)/a]s(t)\,dt \quad (8)$$

where g^* represents complex conjugate of g, the analyzing wavelet, defined on the open time and scale half-plane H, b representing a waveform correlation delay time, "a" representing wavelet frequency or dilation factor and $s(t)$ the signal being processed. Though this definition is concise, in order to understand the physical sense of what information is contained in wavelet transform, it is helpful for structural dynamicists to first consider its Fourier transform counterpart, the Short-Time Fourier transform (STFT) [Flandrin and Rioul, 1990]. The definition of an STFT is

$$F_s(b,a) = \int_{-\infty}^{\infty} s(t)h^*(t-b)\exp(-i2\pi at)\,dt \quad (9)$$

where h^* is the windowing function for the transform. The STFT uses modulated versions of a low pass filter to analyze spectral content [Flandrin and Rioul, 1990]. It is important to understand the restrictions that this form places upon the analyzed signal. The STFT correlates a complex waveform of constant envelope in time with the signal, but changing frequency, meaning that as the frequency is increased, the number of oscillations inside the envelope also increases.

For a large window in time, low frequencies are able to be analyzed; however, poor high frequency localization is also the result. Individual frequency events are poorly defined. If the window is made small, so that high frequencies are successfully localized, bandwidth is small also and resolution on the lower end of the frequency scale is sacrificed. Accuracy also suffers from the fundamental assumption concerning the computation of a Fourier Transform; that the signal is infinite in time, and the window employed represents a period of an infinite signal. This assumption is, of course, patently wrong for many nonstationary signals, including many that would be of interest in engineering science, especially those that are primarily concerned with the start-up of machinery or any transient phenomena.

The wavelet transform has a significantly different structure than the STFT discussed above. Here, a selected analyzing waveform, modified by a given envelope, is defined to have a fixed number of oscillations inside this envelope. See Fig 1. The width of the envelope and the frequency scale together as the frequency is increased to hold the number of oscillations constant. Thus, as frequency is increased, the time envelope of the signal is narrowed. This property gives good resolution in the frequency domain (up to theoretical Nyquist limitations), and good localization in the time domain, since the envelope size, or the length in time of the wavelet directly scales with the frequency of the sinusoid inside the envelope.

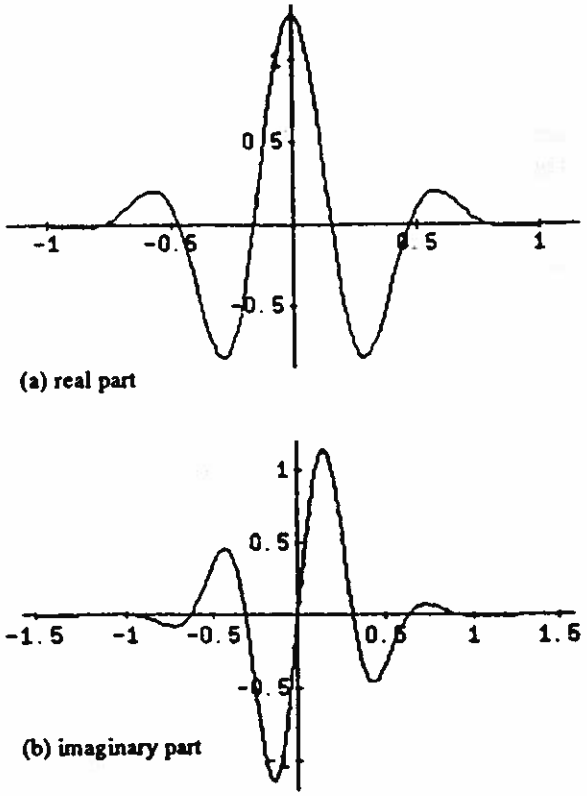

Fig 1. Typical analyzing wavelet.

Because of these properties, the wavelet transform can serve as a sort of signal processing microscope for analyzing local frequency content [Arneodo and Grasseau, 1988]. It is also important to consider the normalization factor placed in the functional form, $a^{-1/2}$. This factor normalizes the autocorrelation of an actual wave packet as shown in Fig 1, thus setting the wavelet transform of a wavelet equal to unity. For structural dynamicists, of more practical interest is a normalization that sets the correlation of a sine wave with a wavelet composed of that sine wave frequency equal to unity. This transforms the normalization to a^{-1}, leaving the preferred functional form to be

$$S(b,a) = a^{-1}\int g^*[(t-b)/a]s(t)\,dt \tag{10}$$

This is the transform used for the calculations in this paper. Because of the form of the transform, use of a different normalization factor will obviously yield different results. One possible modification of the normalization factor might be to deal with fractal signals possessing a certain roll-off in the frequency spectrum [Arneodo and Grasseau, 1988]. The normalization factor could be used to compensate for average trends in the frequency spectrum, leaving only discrete events to be illuminated by the wavelet transform.

Nonstationarity of the signal also becomes less significant in wavelet analysis. Since the wavelet transform is defined locally over a given interval, it does not depend on the long-time behavior of the signal, nor are assumptions as such made in the formulation. This turns out to be important in analyzing transients present in mechanical systems, especially ones with constantly increasing carrier frequencies, as would be encountered in the spin-up of a shaft.

Computational details of the wavelet transform

Since wavelet transform encompasses a wide variety of waveforms meeting certain admissibility conditions that are explained in [Meyer, 1989], it is necessary to design a wavelet that will give the user the information desired to complete the analysis. When considering problems in structural dynamics, the traditional wavelet formulation used is adequate, after consideration of the appropriate normalization. The generating function for the wavelet family used for analysis in this paper is

$$g(c,\tau) = e^{ic\tau}\exp(-\tau^2/2\pi^2) \tag{11}$$

which, upon substitution of the scaled time, $\tau = \omega t/c$ centered about 0 yields

$$g(\omega,t) = e^{i\omega t}\exp[-t^2/2(c\pi/\omega)^2] \tag{12}$$

where $c\pi/\omega$ is the standard deviation of the Gaussian distribution used to modulate the complex waveform, c is a constant used to determine the number of oscillations inside the main body of the Gaussian envelope, and ω is the frequency of the sinusoid being modulated. For the figure in this paper, $c = 1$. The wavelet is set to span the distance of six standard deviations of the Gaussian, thus giving three complete oscillations of the complex sinusoid. The wavelets generated are then correlated with the signal to be analyzed.

Because the signals analyzed are not assumed to be periodic, the analyzing waveforms do not wrap around from the beginning to the end of the signal. Therefore, the waveform correlation magnitude is only formed when the complete waveform can be correlated with the signal. The correlation sequence begins when the left end of the wavelet is aligned with the left end of the time signal, and ends when the right end of the wavelet is aligned with the right end of the time signal. The wavelet correlation magnitude is plotted on the graphs at the time where the center of the wavelet coincides with the time signal. This implementation results in the broad U shape associated with the figures. As the wavelet frequency is increased, the temporal length of the analyzing wavelet shrinks, leaving a much smaller temporal distance between the left side and the center of the analyzing waveform, thus giving the U shape.

BICOHERENCE RESULTS

For many weakly nonlinear systems, nonlinear resonances are often observed at the linearized natural frequency and at twice the natural frequency [Nayfeh and Mook, 1979]. Consequently, Eq (2) with $\Omega = 0.159$ Hz, the first resonance of the system, was examined. F_0 was set at 0.21, the chaos boundary where chaotic oscillations are first observed for the single frequency excitation case [Dowell and Pezeshki, 1986]. Figure 2 shows the phase plane trajectories for φ =

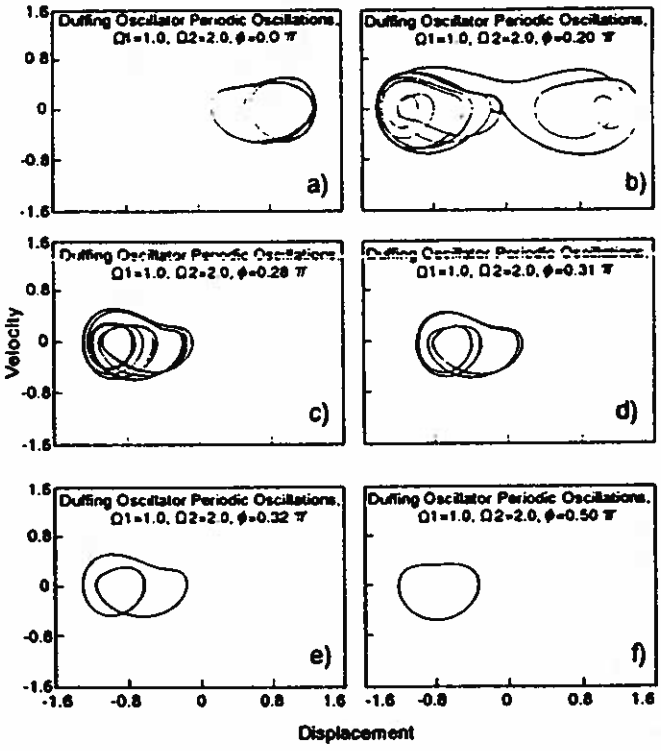

Fig 2. Phase plane trajectories, Eq 2, $F_0 = 0.21$, $\varphi = 0.0$ (a), 0.2 (b), 0.28 (c), 0.31 (d), 0.32 (e), 0.5 (f).

0.0, 0.20, 0.28, 0.31, 0.32, and 0.50. Varying the phase angle for this forcing function produces a classic period doubling sequence (Figs 2f-c), followed by an intermittency crisis into and out of chaos. The period doubling sequence into chaos is almost identical to the single frequency forcing case; see [Dowell and Pezeshki, 1986] for comparison. Power spectra for the respective attractors are shown in Fig 3. As expected, for the power spectra shown in Fig 3a and 3e, a strong subharmonic is present at 1/2 the excitation frequency. The power spectrum shown in Fig 3b is broadband, typical of a chaotic system, and the power spectra shown in Figs 3c and 3d contain the requisite subharmonics for period octupling and period quadrupling.

The cross bicoherence of the input signal relative to the output (Fig 4) for a single period limit cycle (ie Figs 2f, 3f) shows a mechanism that is consistent with the control frequency transferring energy back to the natural frequency, which then redistributes the energy between the harmonics as it had done with the single frequency excitation case [Pezeshki et al, 1990]. A summing interaction is found between $f = 0.159$ Hz, the excitation at the natural frequency, and itself, creating the frequency triad ($f_1 = 0.159$ Hz, $f_2 = 0.159$ Hz, $f_{1+2} = 0.318$ Hz). A differencing interaction is found between the controlling frequency, $f = 0.32$ Hz, and the main excitation, f = 0.159 Hz, creating the frequency triad ($f_1 = 0.318$ Hz, $f_2 = 0.159$ Hz, $f_{1+2} = 0.159$ Hz).

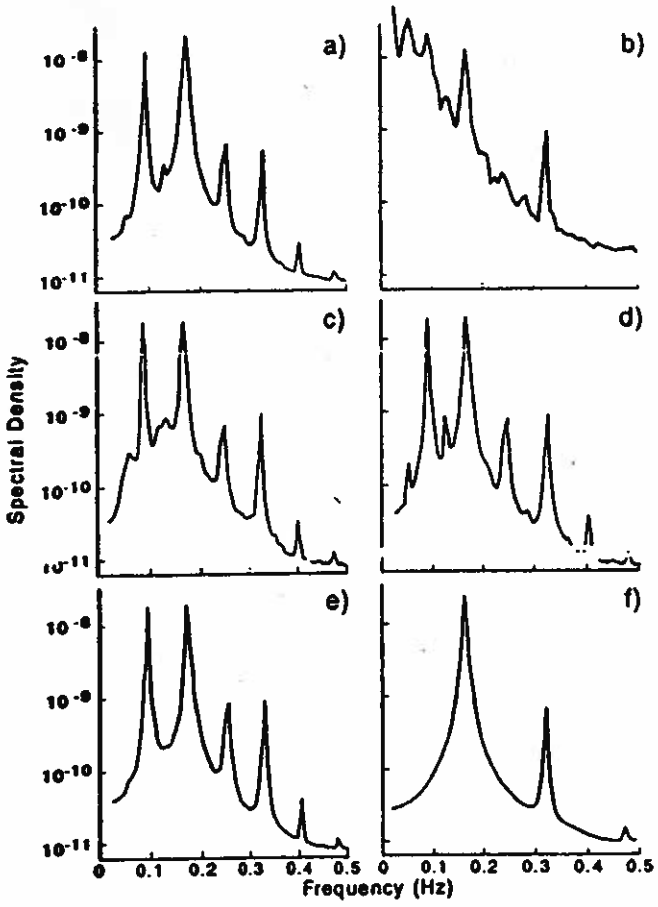

Fig 3. Power spectra, Eq 2, $F_0 = 0.21$, $\varphi = 0.0$ (a), 0.2 (b), 0.28 (c), 0.31 (d), 0.32 (e), 0.5 (f). The units of power are arbitrary.

By varying the phase of the controlling frequency input, an effect is observed whereby the phase of the frequency generated by the differencing interaction between ($f_1 = 0.318$ Hz, $f_2 = 0.159$ Hz, $f_{1+2} = 0.159$ Hz) effectively creates an out-of- phase motion between $f_{1+2} = 0.159$ Hz and the main excitation, also at $f = 0.159$ Hz. This interaction thus enables quenching the chaotic motion by effectively raising or lowering F_0 for the main sinusoidal input. Cases were also run with the phase angle equal to 0.85π and π (not shown). Maximum quenching was observed at 0.85π. The slight phase angle shift from the maximum out-of-phase effect is attributed to the cubic behavior of the system. This offers possibilities for control of nonlinear systems with strong harmonic content by imposing oscillations at frequencies other than the primary.

WAVELET TRANSFORM RESULTS

Figures 5 a,b show an analysis of the transient for Eq (1) for $\gamma = 0.0168$, and $F_0 = 0.05$. The frequency development in the oscillator is clearly illustrated by the wavelet transform. The oscillator initially experiences snap-through dynamics, coupled by a saddle-node intermittency pause, and then settles down to single period motion. By examining the wavelet transform of the transients for the system, one can see a spread of energy at many different frequencies being dissipated and being directed into the primary resonances. Pseudo- chaotic high-frequency energy bursts are followed by a dramatic collapse to the limit cycle attractor, due primarily to the saddle-node instability present in this problem. The steady-state wavelet transform for the low damping case once again assumes the familiar $f = 0.16$ Hz, $f = 0.32$ Hz peak pattern after the transient dies out.

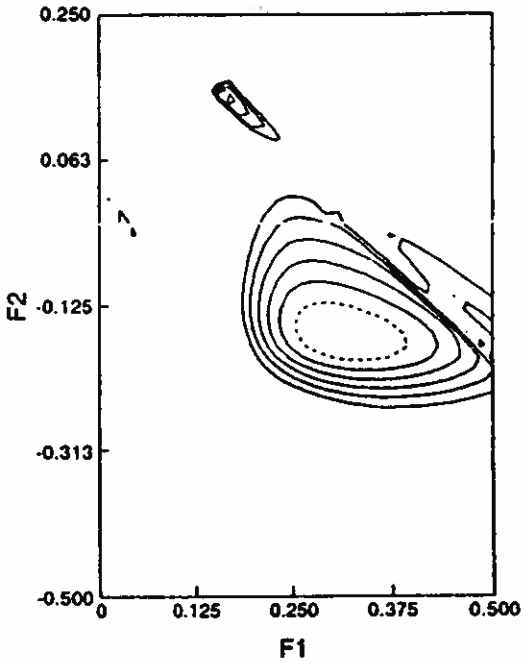

Fig 4. Cross-bicoherence between the forcing function (f_1, f_2) and displacement (f_1+f_2) corresponding to Figs 2f, 3f, and 4f. The minimum contour plotted is $XB = 0.4$, with contours every 0.1. ($F_0 = 0.21$, ($\varphi = 0.5$)

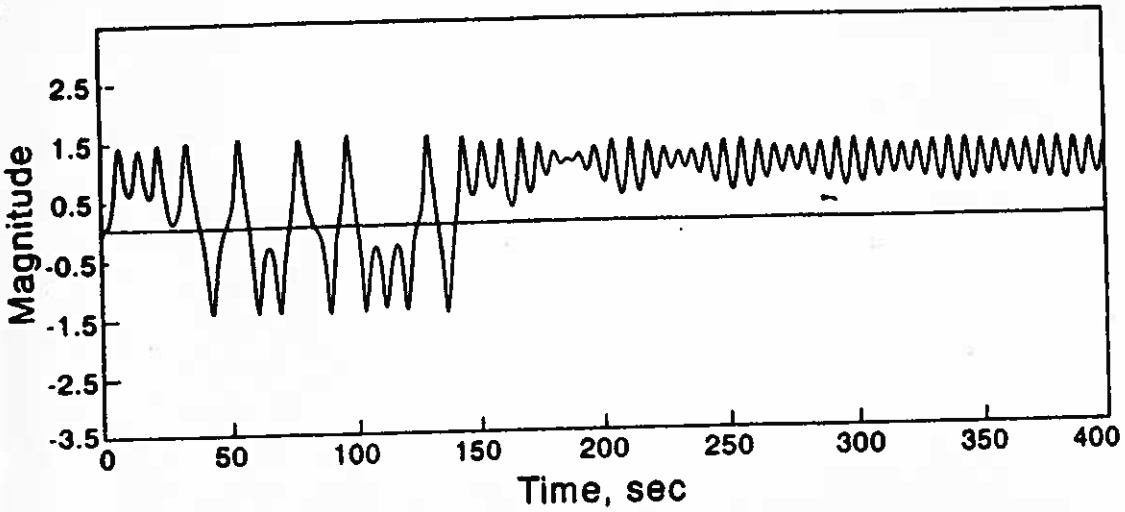

Fig 5. (a) Time history, Duffing equation, $F_0 = 0.05$, $\gamma = 0.0168$, $t = 0 - 400$ s.

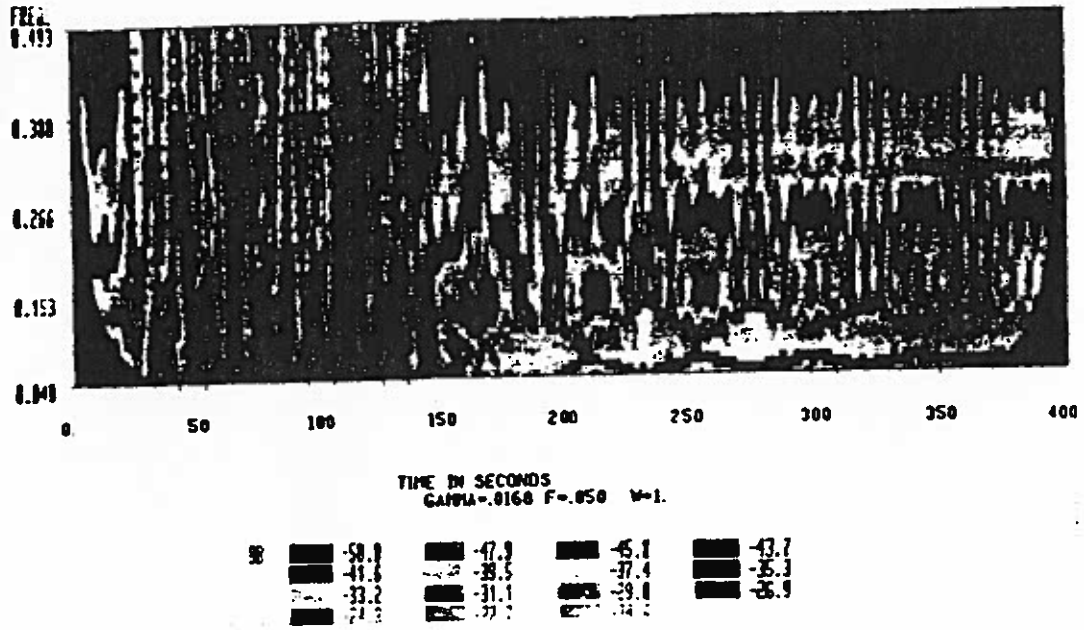

Fig 5. (b) Wavelet transform.

ACKNOWLEDGEMENT

Steve Elgar's research was supported by grants from the Office of Naval Research.

BIBLIOGRAPHY

1. Arneodo A and Grasseau G (Nov 14, 1988), Wavelet Transforms of Multifractals, Phys Rev Lett 61(20), 2281-2284.
2. Daubechies I (1989), in Wavelets Time-Frequency Methods and Phase Space (JM Combes, A Grossman, and Ph Tchamitchan, eds) Springer-Verlag, Berlin, 38-66.
3. David PM and Chapron B (1990), Underwater acoustic signal analysis with wavelet process, *J Acoust Soc Amer* 87(5) 2118-2121.
4. Dowell E and Pezeshki C (1986), On the Understanding of Chaos in Duffing's Equation Including a Comparison With Experiment, *ASME J Appl Mech* 53(1), 5-9.
5. Flandrin P and Rioul O (1990), Affine smoothing of the Wigner-Ville Distribution, IEEE Conference Proceedings of ASSP, 2455-2458.
6. Grossman A, Kronland-Martinet R, and Morlet J (1989), in *Wavelets Time-Frequency Methods and Phase Space* (JM Combes, A Grossman, and Ph Tchamitchan, eds), Springer-Verlag, Berlin, 3-20.
7. Hassleman K, Munk W, MacDonald G, Bispectra of Ocean Waves, in *Time Series Analysis* (ed M Rosenblatt), Wiley (1963), 125-139.
8. Haubrich RA (1965), Earth noises, 5 to 500 millicycles per second, *J Geophys Res* 70, 1415-1427.
9. Kim YC and Powers EJ (1979), Digital Bispectral Analysis and Its Applications to Nonlinear Wave Interactions, *IEEE Trans Plasma Sci* PS7(2), 120-131.
10. Meyer Y (1989), in *Wavelets Time-Frequency Methods and Phase Space* (JM Combes, A Grossman, and Ph Tchamitchin, eds) Springer-Verlag, Berlin, 21-37.
11. Moon F and Holmes PJ (1979), A Magnetoelastic Strange Attractor, *J Sound Vib* 38(6), 275-296.
12. Nayfeh AH and Mook DT (1979), *Nonlinear Oscillations*, Wiley, New York, 161-257, and references therein.
13. Nikias CL and Raghuveer MR (1987), Bispectrum Estimation: A Digital Signal Processing Framework, *IEEE Proc* 75(7), 869-891.
14. Pezeshki C, Elgar S, and Krishna RC (1990), Bispectral Analysis of Systems Possessing Chaotic Motion, *J Sound Vib* 137(3), 357-368.
15. Plaut RH, HaQuang N, and Mook DT (1986), The Influence of an Internal Resonance on Non-linear Structural Vibrations Under Two-Frequency Excitation, *J Sound Vib* 107(2), 309-319.
16. Zavodney LD, Nayfeh AH, and Sanchez NE (1989), The Response of a Single-Degree of Freedom System with Quadratic and Cubic Nonlinearities to a Principal Parametric Resonance, *J Sound Vib* 129(3), 417-442.